ORIGINAL ARTICLE

Remineralizing Potential of Nano-Silver-Fluoride for Tooth Enamel: An Optical Coherence Tomography Analysis

Amitis Vieira Costa e Silva[1], Joás de Araújo Teixeira[2], Paulo Correia de Melo Júnior[3], Maria Goretti de Souza Lima[4], Claudia Cristina Brainer de Oliveira Mota[5], Emery Cleiton Cabral Correia Lins[6], José Ricardo Dias Pereira[7], Anderson Stevens Leônidas Gomes[8], Andréa Gadelha Ribeiro Targino[9], Aronita Rosenblatt[10]

[1]Graduate Program in Dentistry, State University of Pernambuco, Camaragibe, PE, Brazil. 0000-0002-6018-2446
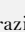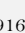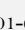[2]Graduate Program in Dentistry, State University of Pernambuco, Camaragibe, PE, Brazil. 0000-0002-9372-0159
[3]Graduate Program in Dentistry, State University of Pernambuco, Camaragibe, PE, Brazil. 0000-0001-6586-1424
[4]Graduate Program in Dentistry, State University of Pernambuco, Camaragibe, PE, Brazil. 0000-0003-2539-2357
[5]Faculty of Dentistry, Center University Tabosa de Almeida, Caruaru, PE, Brazil. 0000-0002-7909-5908
[6]Department of Biomedical Engineering, Federal University of Pernambuco, Recife, PE, Brazil. 0000-0002-7967-6163
[7]School of Dentistry, Federal University of Pernambuco, Recife, PE, Brazil. 0000-0002-9168-3139
[8]Department of Physics, Federal University of Pernambuco, Recife, PE, Brazil. 0000-0001-6536-6570
[9]Department of Dentistry, Federal University of Paraíba, João Pessoa, PB, Brazil. 0000-0001-7492-4714
[10]Graduate Program in Dentistry, State University of Pernambuco, Camaragibe, PE, Brazil. 0000-0003-4606-6374

Author to whom correspondence should be addressed: Joás de Araújo Teixeira, Av. General Newton Cavalcanti, 1650, Tabatinga, Camaragibe, PE, Brazil. 54756-220. Phone: +55 81 3184-7659. E-mail: joasaraujo@hotmail.com.

Abstract

Objective: To evaluate the use of nanosilver fluoride in the enamel remineralization process through optical coherence tomography. **Material and Methods:** All samples were submitted to demineralization process by pH cycling during 14 days and randomly distributed into three groups (n = 11): Nanosilver Fluoride (NSF), Sodium fluoride (NaF), and negative control. Optical coherence tomography images were acquired at three different moments: initial stage (T0), post caries formation (T1), and post pH cycling (T2). The integrity of the enamel surface and the measurement of the volume loss for the tissue after pH cycling in comparison to initial images were obtained from optical coherence tomography images. **Results:** After analyzing the exponential decay of A-scans from each group, it was possible to identify differences in light propagation among samples. In T1 it is not possible to visualize the dentin-enamel junction, probably due to the higher back scattering of the demineralized enamel, which does not allow light to reach the dentin. The decay curves obtained from NaF and nanosilver fluoride groups showed similar behavior, while the negative group showed lower extinction coefficient. **Conclusion:** Nanosilver fluoride showed the best effect against caries compared to conventional fluoride treatments.

Keywords: Nanotechnology; Fluorides; Dental Enamel; Tooth Demineralization.

Introduction

Dental caries is the most prevalent disease of the oral cavity. It occurs due to the demineralization of tooth surfaces by the action of organic acids that originate from the fermentation of carbohydrates by bacteria and organic matrix degradation [1].

Importantly, deciduous teeth have greater permeability, lower bond strength to dental adhesive materials, and lower microhardness when compared to permanent teeth [2]. The lower dimension of the hydroxyapatite lattice, when compared to permanent dentition, also plays an important role in lowering the acid resistance of deciduous teeth [3]. The presence of a thick aprismatic layer in the deciduous enamel at its outermost surface [4] and the fact that the enamel of deciduos teeth is more porous than that of permanent teeth, leading to the milky appearance of the temporary dentition, are also specific characteristics of deciduous teeth. These make them more susceptible to dental caries, and early diagnosis is required to prevent dental caries progression [5].

The demineralization process is dynamic and may be reversed if detected in its early stages. Caries progression occurs when periods of demineralization are more frequent than periods of remineralization. Thus, dental caries occurs when there is an imbalance between demineralization and remineralization. Although small mineral loss may not be clinically visible at earlier stages, the lesion is already present. As demineralization progresses, a whitish area appears as the enamel continues losing minerals [6]. Mineral loss due to disease progression causes visual changes in the tooth surface, starting at the subclinical stage (white spots), followed by cavitation [7].

There has been a search for new methods for early caries detection and optical techniques represent a significant advance in non-invasive imaging methods [8]. Among optically based diagnostic techniques, optical coherence tomography (OCT) allows accurate evaluation of structural mineral loss. It is a non-invasive, non-destructive, non-ionizing, real-time diagnostic method with high sensitivity and specificity in detecting early lesions on smooth and occlusal surfaces [9]. Optical coherence tomography stands out mainly due to its clinical applicability, both for early diagnosis and follow-up of lesion progression, and thus, it was chosen to evaluate the efficiency of the remineralization treatment in the present study. Table 1 includes a literature review on the early diagnosis of dental caries through optical coherence tomography.

Table 1. Studies published in 2013-2017 regarding OCT's application to caries diagnostics.

Authors	Objective	Conclusion
Fried et al. [10]	Quantitative evaluation of enamel remineralization by the CP-OCT System (1,321 nm) *in vivo* before and after the application of fluoride.	OCT was able to clinically monitor enamel remineralization.
Nakagawa [11]	To assess the extent of caries on smooth surfacesvia the SS-OCT System (1,310 nm) *in vitro* as compared to a confocal laser scanning microscope (CLSM)	OCT was suitable for early diagnosis but dependent on clinical experience and the interpretation of the images
Hilsen and Jones [12]	To evaluate and compare three methods, Midwest Caries ID (MID), visual photographic examination (CAM), and *in vitro* CP-OCT (1,310 nm), for use in the detection of enamel demineralization.	MID and CP-OCT were not superior to CAM for use in teledentistry.

Mota et al. [13]	To evaluate morphological changes in caries via the SR-OCT system (930 nm) and compare the results with those achieved via polarized light microscopy *in vitro*.	Equivalent results, but OCT has clinical applicability, and the other method does not.
Gomez et al. [14]	Evaluate the performance of International Caries Detection and Assessment (ICDAS), fiber-optic transillumination (FOTI), SS-OCT (1,315 nm), and quantitative light-induced fluorescence (QLF) in the diagnosis of occlusal caries *in vitro*.	They were equivalent, but visual inspection was sufficient for diagnosis and the determination of caries depth.
Liu and Jones [15]	Evaluate caries in cracks via the SS-OCT System (1,325 nm) as compared to high-resolution x-ray tomography images *in vitro*.	OCT was accurate in evaluating the lesion in terms of depth but not in terms of lateral extension.
Nazari et al. [16]	A longitudinal *in vitro* study evaluated the subsurface enamel lesion progression after 3, 9, and 15 days under hydrated and dry conditions via SS-OCT (1,310 nm).	Hydrated samples are more suitable for evaluating reflectance.
Holtzman et al. [17]	Detection of occlusal caries by means of light fluorescence the International Caries Detection and Assessment System II (ICDAS II), intraoral digital radiography, and SS-OCT (1,310 nm) pre- and post-sealant *in vitro*.	There was betterperformance on the part of OCT for surfaces with and without sealant.
Cara et al. [18]	To evaluate the demineralization of the enamel by the SR-OCT System (930 nm) by calculating the optical attenuation coefficient and the area under the A-scan signal, as well as subsequent comparison with microhardness analysis *in vitro*.	Both methods were able to characterize dental enamel demineralization.
Shimada et al. [19]	To compare SS-OCT images (1,330 nm) and bitewing to assess the depth of proximal caries in the posterior teeth *in vivo*.	OCT responded satisfactorily to enamel, but it had limitations when caries were located in the dentin.
Nakajima et al. [20]	To evaluate SS-OCT (1,330 nm) for use as a diagnostic tool for occlusal caries in deciduous teeth as compared with visual inspection and with confocal laser scanning microscope images *in vitro*.	The results indicate that SS-OCT was able to diagnose caries in primary teeth.
Ibusuki et al. [21]	*In vitro* evaluation of SS-OCT (1,330 nm) use in the quantification of white spot depth in comparison with confocal laser scanning microscopy (CLSM) and light microscopy images, as well as with the ICDAS *in vivo*.	The *in vitro* results of the SS-OCT were compatible with those of microscopy, and *in vivo*, SS-OCT was able to establish the depth of the lesion.
Chan et al. [22]	To evaluate the ability to diagnose the depth of initial lesions *in vitro* through 2D images captured via CP-OCT (1,317 nm) as comparing to histology via polarized light microscopy.	CP-OCT minimized the interference of reflexivity at the surface of the lesion. It was suitable for monitoring *in vivo* and *in vitro* lesions.
Wijesinghe et al. [23]	Evaluation of the evolution of occlusal caries in the enamel *in vitro* via the SD-OCT System (1,310 nm): partially and completely demineralized.	SD-OCT was able to produce quantitative result in all situations.
Chan et al. [24]	To evaluate the ability of the CP-OCT System (1,321 nm) to monitor caries remineralization on smooth surfaces *in vivo*.	CP-OCT was able to evaluate microstructural changes resulting from enamel remineralization.
Lee et al. [25]	Natural enamel caries lesions were assessed *in vitro* via the detection of the surface layer with PS-OCT (1,317 nm), and dehydration rate measurements were performed with NIR reflectance and thermal imaging modalities.	The OCT system was able to measure the caries quantitatively.
Ueno et al. [26]	To evaluate the intensity and attenuation of an SS-OCT signal (1,310 nm) in the dentin and enamel via the variation of mineral density as compared to transverse microradiography images *in vitro*.	There was increased intensity and attenuation of the signal in demineralized and healthy enamel; in dentin, this was true only to a depth of 75 μm.
Maia et al. [27]	Evaluate the morphological differences between sound dental structure and artificially induced white spot lesions in human teeth viaquantitative light-induced fluorescence (QLF) and alterations of the light attenuation coefficient via SR-OCT (930nm) *in vitro*.	Both were suitable. However, SR-OCT revealed more intense optical changes than QLF.

CP-OCT: Cross-Polarization Optical Coherence Tomography; SS-OCT: Swept-Source Optical Coherence Tomography; SR-OCT: Spectral-Radar Optical Coherence Tomography; SD-OCT: Spectral-Domain Optical Coherence Tomography.

Once diagnosed, appropriate procedures are required. Non-invasive treatments for early caries developed significantly since the demineralization mechanism became fully understood. There are several fluoride-based compositions at different concentrations available for topical application. Silver-added preparations based on silver diamine fluoride have also been developed [28-31] as an alternative method of treating caries lesions due to its remineralization effect, which is promoted by the bactericidal action of silver. However, the disadvantage of this approach is that it stains the teeth in black, limiting the aesthetic quality of treatment. With the advent of nanotechnology, specifically nanosilver fluoride (NSF), a compound based on silver nanoparticles, chitosan, and sodium fluoride [32,33], proved to efficiently control dental caries [34-37].

The objective of this study was to evaluate the efficiency of NSF in the enamel remineralization process through optical coherence tomography.

Material and Methods

Specimen Preparation and Experimental Design

Caries lesions were induced in all samples. For the artificial induction of dental caries, 0.05M acetate buffer solution containing 1.28 mM calcium, 0.74 mM phosphate and 0.03 μg fluorine/mL with pH 5.0 was used. Specimens were individually immersed in solution volume of 2 mL/mm2 for 16 hours, remaining at 37ºC during the experimental period and then submitted to demineralization process by pH cycling. Samples were randomly distributed into one of three groups (n = 11) according to the applied treatment (Table 2).

Table 2. Description of the studied groups.

Groups	Type	Remineralizing Solution
G1	Experimental	Nanosilver Fluoride (NSF)
G2	Positive control	Sodium Fluoride (NaF)
G3	Negative control	None

Samples in the negative control group did not receive any remineralizing solution, being only washed in deionized water and kept in phosphate-buffered-saline solution (8 g/L NaCl; 2 g/L KCl; 2 g/L Na2HPO4; 2 g/L KH2PO4; pH = 7.0) for ionic enamel restoration until further OCT images could be acquired at three different moments: initial stage (T0), after chemical induction of caries (T1), and after pH cycling (T2) [38].

Firstly, caries lesion was induced in samples through the application of an acid solution that removed minerals from the enamel to induce the formation of a subsurface lesion. For the artificial induction of dental caries, 0.05 M acetate buffer solution containing 1.28 mM calcium, 0.74 mM phosphate, and 0.03 μg fluorine/mL solution with pH 5.0 was used. Samples were individually immersed in 2 mL/mm2 volume of this solution for 16 hours at 37ºC [38].

Then, pH cycling was carried out over 14 days. The daily procedure included immersing samples in demineralizing solution for 6 hours, followed by 18 hours of immersion in remineralizing

solution. The demineralizing solution was composed of 2.0 mmol/L Ca, 2.0 mmol/L P, and 75 mmol/L acetate buffer and pH 4.4, while the remineralizing solution was composed of 1.5 mmol/L Ca, 0.9 mmol/L P, 130 mmol/L KCl, and 20 mmol/L sodium cacodylate buffer and pH 7.0. All samples were individually washed with deionized water for one minute prior to the application of the test substance (positive control, experimental solution, or negative control). All samples were washed again with deionized water before being immersed in the solution for the new cycle. Solutions were maintained at temperature of 37°C in biological stove [39], as shown in Figure 1.
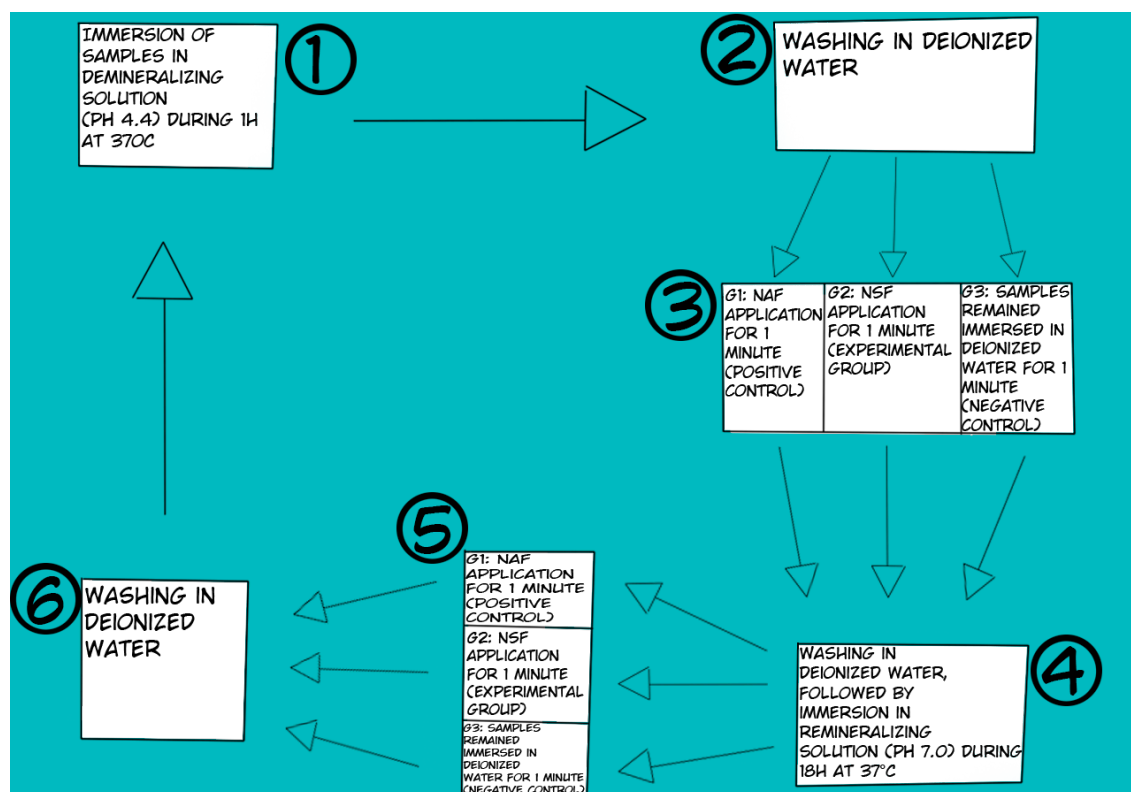

Figure 1. Routine for 24h pH cycling stages, repeated for 14 days.

NSF Synthesis and Characterization

To prepare NSF, 1.0 g of chitosan was dissolved in 200 mL of 2% (V/V) acetic acid solution. The solution was stirred overnight and then vacuum filtered. Later, 60 mL of the chitosan solution were placed in ice bath under stirring. Then, 4.0 mL of 0.012 mol/L silver nitrate solution (AgNO3) were added and left for 30 minutes before adding sodium borohydride (NaBH4).

AgNO3 / NaBH4 mass ratio of 1:6 was maintained via dropwise addition. The reduction of Ag+ ions began immediately, and the solution color changed from colorless to light yellow and finally to red. After 45 minutes in the ice bath, the colloid was removed from the bath and allowed to reach room temperature. NaF was added at concentration of 5,000 ppm and kept under stirring until its complete dissolution. Soon after synthesis, NSF was stored in refrigerator [33,40]. UV-vis spectroscopy and transmission electron microscopy (TEM) were performed for NSF characterization [41].

Optical Coherence Tomography

Specimens were analyzed by optical coherence tomography at three-time points: before chemically-induced caries (T0), after caries induction (T1), and post-cariogenic challenge (T2). A commercial OCT system model (Callisto - Spectral Domain OCT System, Thorlabs Inc., New Jersey, USA) was used [42]. To provide a brief overview, Callisto uses a superluminescent diode laser operating at 930 nm central wavelength as a light source, with 100 nm spectral bandwidth and 3 mW maximum optical power. This model makes images of samples with 7 μm axial resolution when it is immersed in air and 5.3 μm axial resolution when immersed in water. The transverse resolution does not depend on the background, being set at 8 μm. The axial scan rate is 1.2 kHz, which allows capturing two frames per second with 105 dB sensitivity.

Callisto SD-OCT captures data in a matrix of 512 lines x 2,000 columns. The A-scan mode projects Y-axis data as dependent on the deep light penetration, limited to 1.7 mm. The B-scan mode creates proper 2D-OCT images, which are composed of all 2,000 A-scans captured along width of up to 6 mm, corresponding to 1.7 mm maximum depth penetration (in air). A complimentary 3D mode was composed of B-scans captured in a sequence of 250 μm steps, until the complete mapping of surfaces and subsurfaces of samples was achieved. Three-dimensional images allow the user to visualize B-scans along XY, XZ, and YZ planes.

OCT Imaging Analysis

OCT results were processed in ImageJ software (National Institute of Health, USA) [43] with computational routine that averaged 50 user-selected A-scans. In fact, the choice of the region of interest (ROI) is important because it ensures that the analysis is meaningful. For this, the central region of the OCT images of specimens was chosen, where the surface was plane. This allowed the depth of the OCT signal penetration to be similar among the 50 A-scans. This analysis qualitatively examines the changes that occurred in the optical properties of the enamel because the profile of the OCT signal at a certain depth in the sample will be affected by the demineralization and remineralization process. The integrity of the enamel surface and the measurement of the volume loss for the tissue after pH cycling in comparison to initial images were obtained from OCT images.

Ethical Aspects

This experimental in vitro study was carried out with the approval of the Ethics Committee for Research with Humans of the Federal University of Paraiba (CAAE: 48033215.0.0000.5188) and the Declaration of Helsinki.

Results

UV-VIS analysis showed a peak at 400 nm, confirming the presence of silver nanoparticles in the compound, and TEM images showed monodisperse and spherical silver particles with diameter of 8.7 ± 3.1 nm, as shown in Figure 2.
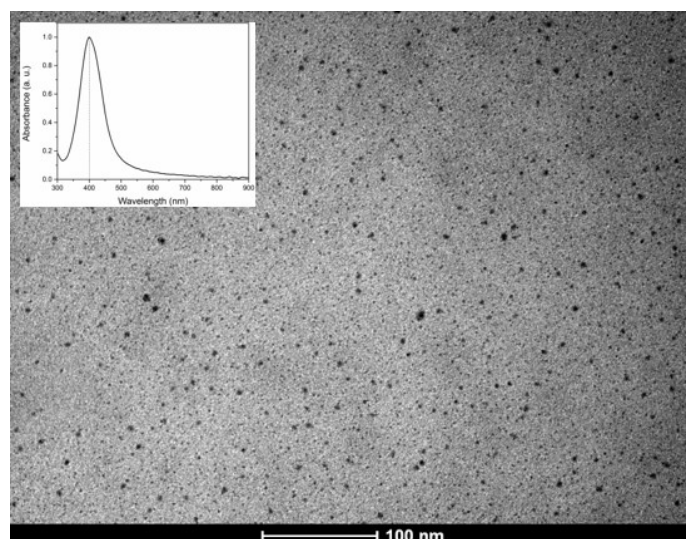
Figure 2. Silver nanoparticles in the NSF validated by transmission electron microscopy image and UV-vis spectrophotometry.

Figure 3 shows a representative image of a sound tooth sample before being submitted to pH cycling. The figure shows the enamel layer over the dentin and a dark line between them, which represents the dentin-enamel junction (DEJ). An A-scan (yellow curve) is shown, in which the tissue interfaces are evidenced by the peaks in the graph.
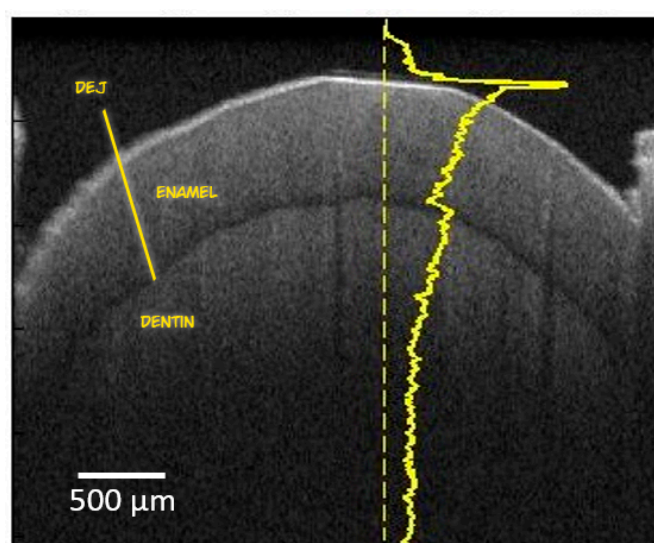

Figure 3. OCT image showing the enamel and dentin layers and also the dentin-enamel junction. These anatomical structures are confirmed by the A-scan of a selected point, presented in the form of yellow lines, showing the peaks of various tissue layers due to the differences in the irrefractive indexes.

Differences can be observed in teeth submitted to cariogenic challenge, as shown in Figure 4. For instance, in T1 images (4b and 4e), it is not possible to visualize the DEJ, probably due to the higher back scattering of the demineralized enamel, which does not allow light to reach the dentin.

By analyzing the exponential decay of A-scans from each group, it is possible to identify differences in light propagation in samples, especially at T2. It was observed that the decay curves

obtained from NaF and NSF show similar behaviors, while the negative control group has lower extinction coefficient (Figure 5).
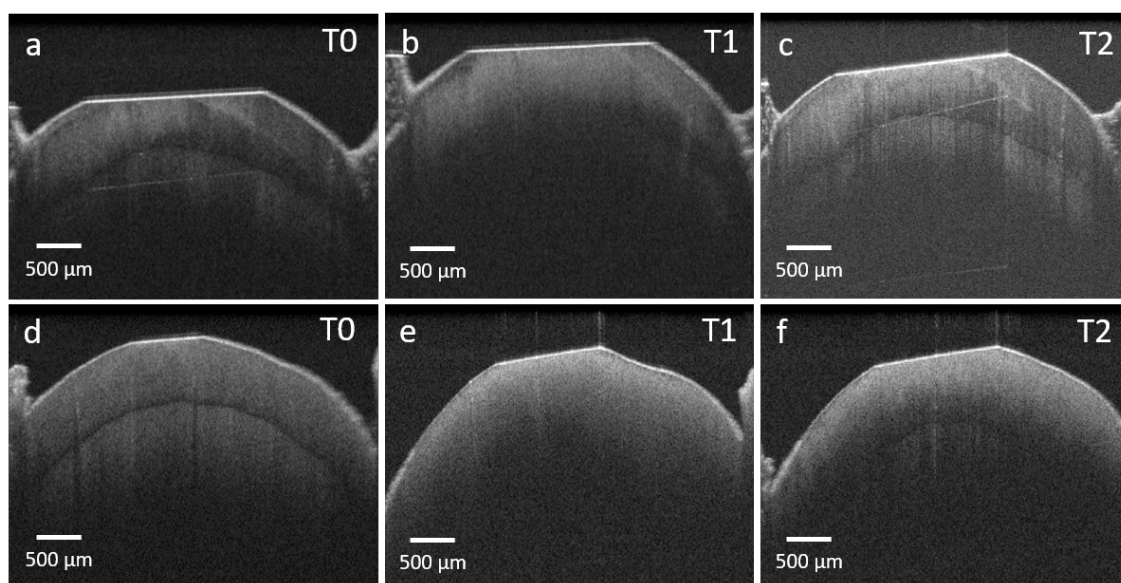

Figure 4. Sequence of images obtained from representative samples at different moments during pH cycling, showing changes in the deciduous teeth. (a), (b), and (c) were obtained from the NSF group, while (d), (e), and (f) were obtained from the negative control group. (a) and (d) show the samples at T0, that is, before the pH cycling. (b) and (e) were taken at T1, and (c) and (f) were taken at the end of T2.
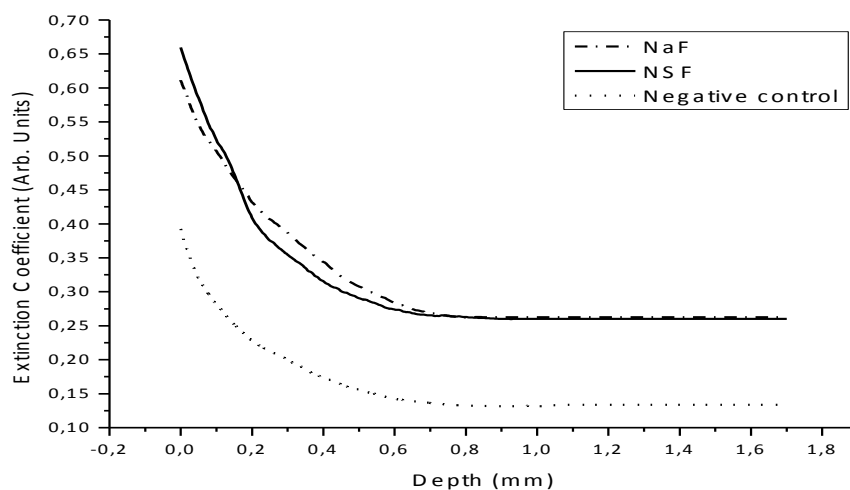

Figure 5. Exponential decay of A-scans obtained from each group – NaF, NSF, and the negative control group – at T2.

Discussion

The use of optical methods for the diagnosis of minimal structural changes has proven to be effective in dental practice and less invasive than other methods. If early diagnosed, caries lesions can

be treated [43-45]. Visual and tactile methods for caries detection and radiographic examination may not be as effective as OCT.

Optical coherence tomography stands out in this context because it is clinically applicable and has high sensitivity and specificity for early diagnosis of caries [17]. In addition, it is capable of detecting structural changes via qualitative and quantitative analysis [46]. It is important to note that OCT has limitations, specifically low penetration capacity due to signal attenuation and scattering. However, given the enamel thickness (on the order of 1-2 mm), it is quite appropriate. In the presence of caries, greater scattering can further reduce image quality at greater depths. Another important consideration regarding image quality is the technical parameters of the OCT equipment used, such as central wavelength of the light source and bandwidth, which are important in determining the axial resolution [47].

Another factor to be considered is that depending on the wavelength, there is likely greater variation in the total attenuation of the signal in the enamel than in the dentin. In this context, an OCT image has good quality when there is high axial resolution, in addition to good contrast and reasonable depth penetration. Thus, based on the characteristics of the examined object, parameters such as central wavelength, bandwidth, and optical instrumentation must be adjusted so that the advantages of this system overcome disadvantages.

The studies shown in Table 1 describe various OCT systems operating at different wavelengths that are used for the diagnosis of changes in tooth enamel. Short-wavelength OCT systems, such as our 930 nm or 900 nm systems, are ideal for high-resolution imaging as compared to systems with a 1,300 nm center wavelength [43]. Thus, for the in vitro evaluation of enamel demineralization, the 930nm SD-OCT system is superior for the diagnosis of structural enamel alterations.

Regarding the results obtained, Figure 3 shows an A-scan superimposed over a representative OCT image captured from a healthy deciduous tooth. This overlap allows observing the sensitivity of the technique in detecting the light propagation that occurs during the penetration of the incident beam. Along the path of the A-scan, it is possible to observe the presence of two peaks, the first is at the air–enamel interface and the second is at the enamel–dentin interface. These peaks indicate changes in the refraction index that occur when light propagates into a new and different medium. This is important in evaluating the penetrative behavior of light during A-scan formation.

In this study, NSF was tested as a dental enamel remineralizing agent. It was compared to NaF and to a negative control via OCT images. Figure 4 shows the light propagation behavior from the enamel surface to the dentin in the various phases in the NSF group and negative control group. It could be observed that on the enamel surface, in phases T0 (Figure 4a and 4d) and T2 (Figure 4c), it was possible to observe the entire length of the enamel layer, including the differentiation between prismatic and aprismatic layers, the enamel/dentin junction, and the dentin. In phase T1 (Figure 4b), it was not possible to differentiate the enamel from the dentin. Similar results were observed in

phases T1 (Figure 4e) and T2 (Figure 4f) for the negative control group. This behavior can be explained by enamel demineralization. In this situation, there is an intense increase in backscattering in this region, so the light does not reach deeper layers, where the dentine is found. This is justified by the caries induction in the enamel in phase T1 in all three groups.

This fact corroborates literature findings, suggesting that in the presence of caries, there is greater scattering due to the modification of the scattering properties in carious enamel, which can further reduce image quality at greater depths [43]. In the negative control group, this intense back scattering was repeated in T2 (Figure 4f), whereas in NSF and NaF groups, there was a reversal, and backscattering was decreased in T2 (Figure 4c). In the negative control group, lower backscattering reduction was observed, because this group was not able to remineralize induced caries lesions. Figure 5 shows the performance of enamel remineralization based on the analysis of A-scans obtained from OCT images. NaF and NSF groups showed similar behavior during the A-scan analysis of the T2 remineralization pattern, which demonstrates the equivalent abilities of these fluorides to remineralize the demineralized enamel. On the other hand, A-scan of the control group presented much lower scattering coefficient when compared to the remineralization pattern observed in T2.

Regarding the performance of NSF, the results indicate that silver nanoparticles do not interfere with the action of fluoride. This can be explained by the inherent ionic stability of silver [32]. This finding is especially important in deciduous teeth due to a peculiar feature of their enamel: these teeth are less thick and have enamel layer that corresponds to almost half the size of the permanent teeth, and is more permeable and less hard than that of permanent teeth [2,3]. Decidious enamel is also prone to the progression of caries, which occurs about 1.5 times faster than in permanent teeth [9]. In contrast, it is important to emphasize that despite these disadvantages in relation to permanent teeth, deciduous teeth are more sensitive to fluoride treatment. This may be explained by the greater permeability of the deciduous enamel, which is about 150 times greater than in permanent teeth, allowing the fluoride diffusion [2]. The use of NSF for enamel remineralization in deciduous teeth may enhance the performance of fluoride with antimicrobial action of silver nanoparticles added to this compound. Since this enamel is more sensitive to acid action, the bactericidal potential of silver will be able to increase the effect of fluoride without causing staining, while preserving the remineralization potential [34,35,48-50].

Conclusion

Nanosilver fluoride is as efficient as NaF in remineralizing dental enamel and the SD-OCT system is sensitive for the evaluation of enamel remineralization in deciduous teeth based on A-scan evaluation of images obtained.

Conflict of Interest: The authors declare no conflicts of interest.

References

[1] Nakornchai S, Atsawasuwanb P, Kitamurac E, Suraritd R, Yamauchi M. Partial biochemical characterisation of collagen in carious dentin of human primary teeth. Arch Oral Biol 2004; 49(4):267-73. https://doi.org/10.1016/j.archoralbio.2003.11.003

[2] Oliveira MAHM, Torres CP, Gomes-Silva JM, Chinelatti MA, Menezes FCH, Palma-Dibb RG, Borsatto MC. Microstructure and mineral composition of dental enamel of permanent and deciduous teeth. Microsc Res Tech 2010; 73(5):572-7. https://doi.org/10.1002/jemt.20796

[3] Low LM, Duraman N, Mahmood U. Mapping the structure, composition and mechanical properties of human teeth. Mater Sci Engineering 2008; 28(2):243-7. https://doi.org/10.1016/j.msec.2006.12.013

[4] Fava M, Watanabe I, Moraes FF, Costa LRRS. Prismless enamel in human non erupted deciduous molar teeth: A scanning eletron microscopic study. Rev Odontol Univ São Paulo 1997; 11(4):239-43. https://doi.org/10.1590/S0103-06631997000400003

[5] Silverstone LM. The histopathology of early approximal caries in the enamel of primary teeth. ASDC J Dent Child 1970; 37(3):201-10.

[6] Núñez DP, Bacallao LG. Bioquímica de la caries dental. Rev Haban Cienc Méd 2012; 9(2):156-66. [In Spanish]

[7] Cury JA, Tenuta LMA. Enamel remineralization: Controlling the caries disease or treating early caries lesions? Braz Oral Res 2009; 23(Suppl1):23-30. https://doi.org/10.1590/S1806-83242009000500005

[8] Rodrigues JA, Diniz MB, Josgrilberg EB, Cordeiro RL. In vitro comparison of laser fluorescence performance with visual examination for detection of occlusal caries in permanent and primary molars. Lasers Med Sci 2009; 24(4):501-6. https://doi.org/10.1007/s10103-008-0552-4

[9] Amaechi BT. Emerging technologies for diagnosis of dental caries: The road so far. J Appl Phys 2009; 105:102047. https://doi.org/10.1063/1.3116632

[10] Fried D, Staninec M, Darling CL, Chan KH, Pelzner RB. Clinical monitoring of early caries lesions using cross polarization optical coherence tomography. Proc SPIE Int Soc Opt Eng 2013; 8566. https://doi.org/10.1117/12.2011014

[11] Nakagawa H, Sadrb A, Shimada Y, Tagami J, Sumi Y. Validation of swept source optical coherence tomography (SS-OCT) for the diagnosis of smooth surface caries in vitro. J Dent 2013; 41(1):80-9. https://doi.org/10.1016/j.jdent.2012.10.007

[12] Hilsen ZV, Jones RS. Comparing potential early caries assessment methods for teledentistry. BMC Oral Health 2013; 13:16. https://doi.org/10.1186/1472-6831-13-16

[13] Mota CCBO, Gueiros LA, Maia AMA, Santos-Silva AR, Gomes ASL, Alves FA, et al. Optical coherence tomography as an auxiliary tool for the screening of radiation-related caries. Photomed Laser Surg 2013; 31(7):301-6. https://doi.org/10.1089/pho.2012.3415

[14] Gomez J, Zakian C, Salsone S, Pinto SCS, Taylora A, Pretty LA, Ellwood R. In vitro performance of different methods in detecting occlusal caries lesions. J Dent 2013; 41(2):180-6. https://doi.org/10.1016/j.jdent.2012.11.003

[15] Liu X, Jones RS. Evaluating a novel fissure caries model using swept source optical coherence tomography. Dent Mater J 2013; 32(6):906-12. https://doi.org/10.4012/dmj.2013-075

[16] Nazari A, Sadr A, Campillo-Funollet M, Nakashima S, Shimada Y, Tagami J, Sumi Y. Effect of hydration on assessment of early enamel lesion using swept-source optical coherence tomography. J Biophotonics 2013; 6(2):171-7. https://doi.org/10.1002/jbio.201200012

[17] Holtzman JS, Ballantine J, Fontana M, Wang A, Calantog A, Benavides E, et al. Assessment of early occlusal caries pre- and post- sealant application – An imaging approach. Lasers Surg Med 2014; 46(6):499-507. https://doi.org/10.1002/lsm.22249

[18] Cara ACB, Zezell DM, Ana PA, Maldonado EP, Freitas AZ. Evaluation of two quantitative analysis methods of optical coherence tomography for detection of enamel demineralization and comparison with microhardness. Lasers Surg Med 2014; 46(9):666-71. https://doi.org/10.1002/lsm.22292

[19] Shimada Y, Nakagawa H, Sadr A, Wada I, Nakajima M, Nikaido T, et al. Noninvasive cross-sectional imaging of proximal caries using swept-source optical coherence tomography (SS-OCT) in vivo. J Biophotonics 2014; 7(7):506-13. https://doi.org/10.1002/jbio.201200210

[20] Nakajima Y, Shimada Y, Sadr A, Wada I, Miyashin M, Takagi Y, et al. Detection of occlusal caries in primary teeth using swept source optical coherence tomography. J Biomed Opt 2014; 19(1):16020. https://doi.org/10.1117/1.JBO.19.1.016020

[21] Ibusuki T, KitasakoY, Sadr A, Shimada Y, Sumi Y, Tagam J. Observation of white spot lesions using swept source optical coherence tomography (SS-OCT): In vitro and in vivo study. Dent Mater J 2015; 34(4):545-52. https://doi.org/10.4012/dmj.2015-058

[22] Chan KH, Chan AC, Fried WF, Simon JC, Darling CL, Fried D. Use of 2D images of depth and integrated reflectivity to represent the severity of demineralization in cross-polarization optical coherence tomography. J Biophotonics 2015; 8:36-45. https://doi.org/10.1002/jbio.201300137

[23] Wijesinghe RE, Cho NH, Park K, Jeon M, Kim J. Bio-photonic detection and quantitative evaluation method for the progression of dental caries using optical frequency-domain imaging method. Sensors 2016; 16(12):E2076. https://doi.org/10.3390/s16122076

[24] Chan KH, Tom H, Lee RC, Kang H, Simon JC, Staninec M, et al. Clinical monitoring of smooth surface enamel lesions using CP-OCT during on surgical intervention. Lasers Surg Med 2016; 48(10):915-23. https://doi.org/10.1002/lsm.22500

[25] Lee RC, Staninec M, Le O, Fried D. Infrared methods for assessment of the activity of natural enamel caries lesions. IEEE J Sel Top Quantum Electron 2016; 22(3):6803609. https://doi.org/10.1109/JSTQE.2016.2542481

[26] Ueno T, Shimada Y, Matin K, Zhou Y, Wada I, Sadr A, Sumi Y, Tagami J. Optical analysis of enamel and dentin caries in relation to mineral density using swept-source optical coherence tomography. J Med Imaging 2016; 3(3):035507. https://doi.org/10.1117/1.JMI.3.3.035507

[27] Maia AMA, Freitas AZ, Campello SL, Gomes ASL, Karlsson L. Evaluation of dental enamel caries assessment using quantitative light induced fluorescence and optical coherence tomography. J Biophotonics 2016; 9(6):596-602. https://doi.org/10.1002/jbio.201500111

[28] Robinson C, Shore RC, Brookes SJ, Strafford S, Wood SR, Kirkham J. The chemistry of enamel caries. Crit Rev Oral Biol Med 2000; 11(4):481-95.

[29] Rosin-Grget K, Peros K, Sutej I, Basic K. The cariostatic mechanisms of fluoride. Acta Med Acad 2013; 42(2):179-88. https://doi.org/10.5644/ama2006-124.85

[30] Tenuta LM, Cury JA. Fluoride: Its role in dentistry. Braz Oral Res 2010; 24(Suppl 1):9-17. https://doi.org/10.1590/S1806-83242010000500003

[31] Ijaz S, Croucher RE, Marinho VC. Systematic reviews of topical fluorides for dental caries: A review of reporting practice. Caries Res 2010; 44(6):579-92. https://doi.org/10.1159/000322132

[32] Noronha VT, Amauri JP, Durán G, Galembeck A, Cogo-Müller K, Franz-Montan M, Durán N. Silver nanoparticles in dentistry. Dent Mater 2017; 33(10):1110-26. https://doi.org/10.1016/j.dental.2017.07.002

[33] Wei L, Lu J, Xu H, Patel A, Chen ZS, Chen G. Silver nanoparticles: Synthesis, properties, and therapeutic applications. Drug Discov Today 2015; 20(5):595-601. https://doi.org/10.1016/j.drudis.2014.11.014

[34] Targino AG, Flores MA, dos Santos Junior VE, de Godoy Bené Bezerra F, de Luna Freire H, Galembeck A, Rosenblatt A. An innovative approach to treating dental decay in children. A new anti-caries agent. J Mater Sci Mater Med 2014; 25(8):2041-7. https://doi.org/10.1007/s10856-014-5221-5

[35] Santos Jr VE, Vasconcelos Filho A, Targino AGR, Flores MAP, Galembeck A, Caldas Jr AF, et al. A new "silver-Bullet" to treat caries in children – nano silver fluoride: a randomised clinical trial. J Dent 2014; 42(8):945-51. https://doi.org/10.1016/j.jdent.2014.05.017

[36] Rabea El, Badawy ME, Stevens CV, Smagghe G, Steurbaut W. Chitosan as antimicrobial agent: Applications and mode of action. Biomacromolecules 2003; 4(6):1457-65. https://doi.org/10.1021/bm034130m

[37] Fu J, Ji J, Fan D, Shen J. Construction of antibacterial multilayer films containing nano silver via layer-by-layer assembly of heparin and chitosan-silver ions complex. J Biomed Mater Res A 2006; 79(3):665-74. https://doi.org/10.1002/jbm.a.30819

[38] Alexandria AKF, Valença AMG, Lima SJG Nóbrega CBC, Lima AL, Claudino LV. In vitro evaluation of the demineralization of bovine enamel subjected to pH and immersion time variations in caries-inducing solution. Pesqui Bras Odontopediatria Clin Integr 2008; 8(2):233-8. https://doi.org/10.4034/1519.0501.2008.0082.0018

[39] Stookey GK, Featherstone JD, Rapozo-Hilo M, Schemehorn BR, Williams RA, Baker RA, et al. The Featherstone laboratory pH cycling model: A prospective, multisite validation exercise. Am J Dent 2011; 24(5):322-8.

[40] Bin Ahmad M, Lim JJ, Shameli K, Ibrahim NA, Tay MY. Synthesis of silver nanoparticles in chitosan, gelatin and chitosan/gelatin bionanocomposites by a chemical reducing agent and their characterization. Molecules 2011; 16(9):7237-48. https://doi.org/10.3390/molecules16097237

[41] Freire PL, Albuquerque AJ, Farias IA, da Silva TG, Aguiar JS, Galembeck A, et al. Antimicrobial and cytotoxicity evaluation of colloidal chitosan – silver nanoparticles – fluoride nanocomposites. Int J Biol Macromol 2016; 93(Pt A):896-903. https://doi.org/10.1016/j.ijbiomac.2016.09.052

[42] Mota CCBO, Fernandes LO, Cimões R, Gomes ASL. Non-invasive periodontal probing through fourier-domain optical coherence tomography. J Periodontol 2015; 86(9):1087-94. https://doi.org/10.1902/jop.2015.150047

[43] Schneider H, Park KJ, Häfer M, Rüger C, Schmalz G, Krause F, et al. Dental applications of optical coherence tomography (OCT) in cariology. Appl Sci 2017; 7(5):472. https://doi.org/10.3390/app7050472

[44] Abdullah Z, John J. Minimally invasive treatment of white spot lesions - A systematic review. Oral Health Prev Dent 2016; 14(3):197-205. https://doi.org/10.3290/j.ohpd.a35745

[45] Mandurah MM, Sadr A, Shimada Y, Kitasako Y, Nakashima S, Bakhsh TA. Monitoring remineralization of enamel subsurface lesions by optical coherence tomography. J Biomed Opt 2013; 18(4):046006. https://doi.org/10.1117/1.JBO.18.4.046006

[46] Schneider H, Park KJ, Rueger C, Ziebolz D, Krause F, Haak R. Imaging resin infiltration into non-cavitated carious lesions by optical coherence tomography. J Dent 2017; 60:94-8. https://doi.org/10.1016/j.jdent.2017.03.004

[47] Ishida S, Nishizawa N. Quantitative comparison of contrast and imaging depth of ultrahigh-resolution optical coherence tomography images in 800–1700 nm wavelength region. Biomed Opt Express 2012; 3(2):282-94. https://doi.org/10.1364/BOE.3.000282

[48] Durán N, Durán M, de Jesus MB, Seabra AB, Fávaro WJ, Nakazato G. Silver nanoparticles: A new view on mechanistic aspects on antimicrobial activity. Nanomedicine 2016; 12(3):789-99. https://doi.org/10.1016/j.nano.2015.11.016

[49] Hernández-Sierra JF, Ruiz F, Pena DC, Martínez-Gutiérrez F, Martínez AE, Guillén AJ, et al. The antimicrobial sensitivity of Streptococcus mutans to nanoparticles of silver, zinc oxide, and gold. Nanomedicine 2008; 4(3):237-40. https://doi.org/10.1016/j.nano.2008.04.005

[50] Espinosa-Cristobal LF, Martinez-Castanon A, Martinez-Maartinez RE, Loyola-Rodriguez JP. Antibacterial effect of silver silver nanoparticles against Streptococcus mutans. Mater Lett 2009; 63(29):2603-6. https://doi.org/10.1016/j.matlet.2009.09.018